

# Fission Cross-Section Measurements of the Odd-Odd Isotopes $^{232}\text{Pa}$ , $^{238}\text{Np}$ , and $^{236}\text{Np}$

Y. Danon\*

*Rensselaer Polytechnic Institute, Department of Nuclear Engineering and Engineering Physics  
Troy, New York 12180*

M. S. Moore, P. E. Koehler,† P. E. Littleton, G. G. Miller, M. A. Ott, L. J. Rowton,  
W. A. Taylor, J. B. Wilhelmy, and M. A. Yates

*Los Alamos National Laboratory, P.O. Box 1663, Los Alamos, New Mexico 87545*

A. D. Carlson

*National Institute for Standards and Technology, Gaithersburg, Maryland 20899*

N. W. Hill

*Oak Ridge National Laboratory, Oak Ridge, Tennessee 37831*

and

R. Harper and R. Hilko

*EG&G Energy Measurements, Los Alamos, New Mexico 87544*

*Received December 21, 1995*

*Accepted March 9, 1996*

**Abstract**—*Transmutation of actinide waste into fission products could be enhanced by using resonance fission of odd-odd target materials; those of interest are  $^{232}\text{Pa}$ ,  $^{238}\text{Np}$ , and  $^{242}\text{Am}$ . Fission cross-section measurements of two of these short-lived materials were performed at Los Alamos National Laboratory. Samples were produced by the  $(d,2n)$  reaction in the Los Alamos Ion Beam Facility followed by fast radiochemistry to separate the odd-odd target of interest. The fission cross section of the nanogram samples was measured in a high intensity pulsed neutron beam produced by 800-MeV proton spallation. Using this procedure, the fission cross sections of the 1.3-day  $^{232}\text{Pa}$  and 2.1-day  $^{238}\text{Np}$  were successfully measured in the energy range from 0.01 eV to 50 keV. The fission cross section of the relatively long-life isotope  $^{236}\text{Np}$  was also measured in the same system while the short half-life isotopes were being prepared. The results and resonance analysis are presented.*

## I. INTRODUCTION

Following the suggestion by Bowman et al.<sup>1</sup> that the transmutation of actinide waste into fission prod-

ucts may be enhanced by using thermal and resonance fission in odd-odd nuclei, it became clear that there was an urgent need to know the resonance properties of the nuclides of interest. The measurements of the fission cross section of isotopes with half-lives of a few days require a neutron beam of very high intensity but of modest resolution. The facility that is probably the best in the world for such measurements is the Los Alamos Neutron Science Center (LANSCE), which uses

---

\*Current address: Nuclear Research Center-Negev, P.O. Box 9001, Beer-Sheva, Israel.

†Current address: Oak Ridge National Laboratory, Oak Ridge, Tennessee 37831.

moderated spallation-neutron pulses from the proton storage ring (PSR), driven by 800-MeV protons from the Los Alamos Meson Physics Facility (LAMPF).

The method of choice for producing sample material for these measurements is by neutron irradiation of isotopes with mass number  $A-1$  in a high flux thermal reactor. We intended, at the time that we began planning these measurements, that this method would be used. If we assume a modest  $10\ \mu\text{g}$  of  $^{231}\text{Pa}$ ,  $^{237}\text{Np}$ , or  $^{241}\text{Am}$  as the starting material, and irradiate it in a thermal flux of  $6 \times 10^{13}\ \text{n/cm}^2 \cdot \text{s}$  for one half-life of the isotope of interest, we obtain 20 to 30 ng, which is quite an adequate amount of sample. (As it turns out, the solution of the Bateman equation for all three of the targets of interest gives roughly the same answer, and the amount of material produced is very nearly proportional to the reactor flux at these relatively low levels.) At the time we planned the measurement, the Omega West Reactor (OWR) at Los Alamos National Laboratory (LANL) was fully operational, and the  $6 \times 10^{13}\ \text{n/cm}^2 \cdot \text{s}$  flux level was readily obtainable in the pneumatic rabbit irradiation ports. By the time the 1993 LAMPF/PSR cycle began, however, the OWR had been shut down for extended repair. We considered two possible alternatives: the Advanced Test Reactor (ATR) at Idaho National Engineering Laboratory, with a thermal flux of  $6 \times 10^{14}\ \text{n/cm}^2 \cdot \text{s}$ , or the Annular Core Research Reactor (ACRR) at Sandia National Laboratories, which was configured to give  $\sim 4 \times 10^{12}\ \text{n/cm}^2 \cdot \text{s}$  below 1 eV. The ACRR is clearly less than optimal, but the main reason we chose a much more exotic method of producing the sample was because of logistics. Moving the irradiated material on public highways, or, in the case of the ATR, by aircraft to Los Alamos in a reasonable time period after the irradiation, was not easy. We chose to avoid the transportation problem by producing the odd-odd fissile isotopes on site, i.e., at LANL, by charged-particle irradiation at the Los Alamos Ion Beam Facility (IBF).

Preliminary results<sup>2</sup> and application of the measured data to the accelerator transmutation of waste<sup>3</sup> (ATW) were previously presented. This paper extends the resonance analysis treatment and includes the  $^{236}\text{Np}$  measurement that was carried out at the same time with the same experimental arrangement.

## II. SAMPLE PRODUCTION

The first step in producing the required samples was to measure the cross sections for  $(p, xn)$  and  $(d, xn)$  reactions as a function of the energy of the charged particle for  $^{232}\text{Th}$  and  $^{238}\text{U}$  targets. The cross sections for  $(p, n)$  and  $(p, 3n)$  reactions with  $^{232}\text{Th}$  are shown in Fig. 1. We found that the  $(p, n)$  and  $(p, 3n)$  cross sections of  $^{238}\text{U}$  show qualitatively the same energy dependence but are  $\sim 20\%$  lower. Clearly, however, protons are not suitable for producing the isotopes of

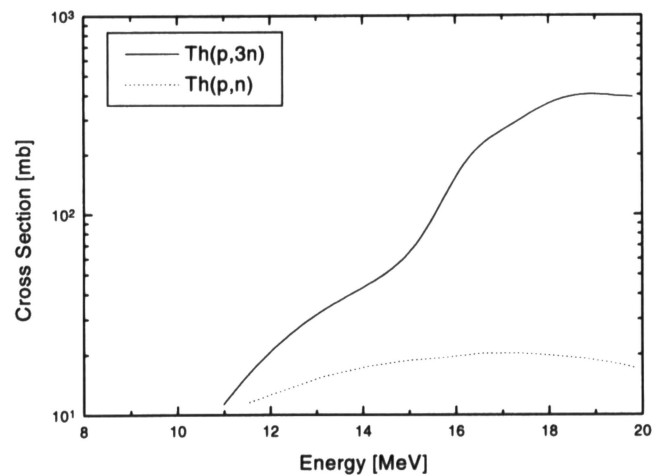


Fig. 1. Measured cross sections in millibarns for  $^{232}\text{Th}(p, n)$  by the dotted line and for  $^{232}\text{Th}(p, 3n)$  by the solid line. The measured cross sections for proton irradiation of  $^{238}\text{U}$  have the same shape but are 20% lower.

interest to the ATW program; the odd-odd isotopes  $^{230}\text{Pa}$  and  $^{236}\text{Np}$  are produced with up to ten times more efficiency than the isotopes of primary interest,  $^{232}\text{Pa}$  and  $^{238}\text{Np}$ , and are expected to have even larger fission cross sections for low energy neutrons. The next step was to measure the cross sections of  $^{232}\text{Th}$  and  $^{238}\text{U}$  for deuterons. The results, shown in Fig. 2 for  $^{232}\text{Th}$ , suggest that this would give an adequate sample. Even though the  $(d, n)$  cross section is about four times larger than the  $(d, 2n)$  cross section, neither  $^{233}\text{Pa}$  nor  $^{239}\text{Np}$  is expected to have an appreciable neutron-induced fission cross section, and the fission cross sections of their decay products,  $^{233}\text{U}$  and  $^{239}\text{Pu}$ , are well

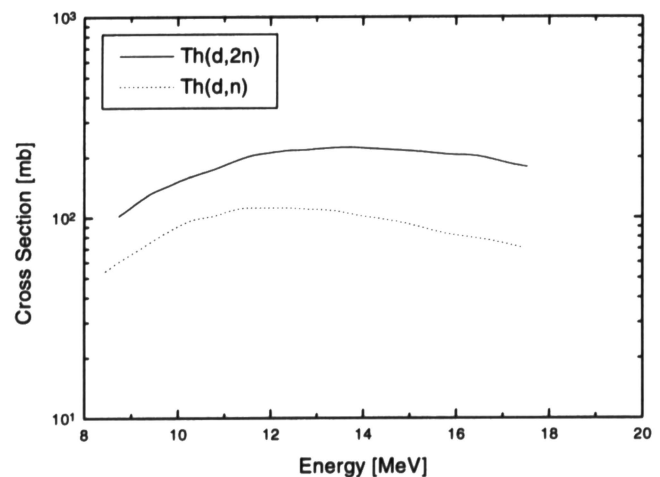


Fig. 2. Measured cross sections in millibarns for  $^{232}\text{Th}(d, n)$  by the dotted line and for  $^{232}\text{Th}(d, 2n)$  by the solid line. The measured deuteron cross sections for irradiation of  $^{238}\text{U}$  have roughly the same shape but are 50% lower.

known. In fact, their presence is an advantage in that it provides a means of normalizing the measurement.

We carried out one successful measurement of  $^{232}\text{Pa}$  and two of  $^{238}\text{Np}$ . Each of these consisted of irradiation of thorium or  $^{238}\text{U}$  at the IBF, followed by fast chemistry to separate the protactinium or neptunium, which was then deposited on a backing, assembled into a fission chamber, transported to the LANSCE facility, and inserted into the neutron beam. The procedure was not without problems. In particular, the  $^{238}\text{U}$  foils occasionally burned through if the deuteron currents were too high or if the beam spots were too sharply focused, which led to catastrophic vacuum failure and contamination of the IBF beamline. As a result, we did not attempt to field a sample of 16-h  $^{242}\text{gAm}$ , which could have been produced by deuteron irradiation of  $^{242}\text{Pu}$ .

The long-lived  $^{236}\text{Np}$  sample had been produced several years earlier by deuteron irradiation of  $^{235}\text{U}$ . A fission foil,<sup>a</sup> consisting of 11 ng of the material, was electroplated on a titanium backing as an additional measurement of interest to nuclear systematics.

### III. FISSION CROSS-SECTION MEASUREMENTS

A compensated ionization chamber with five parallel plates was used to measure the time-dependent fission rates; it is illustrated in Fig. 3. In this chamber, the plate spacing was 0.5 cm. The first and last plates were the anodes, at +400 V. The second and fourth plates were the cathodes, at ground potential, from which the fission fragments pulses were taken. On the fourth plate was a deposit of  $\sim 400$  ng of  $^{235}\text{U}$  that served as a flux monitor. On the second plate was the short-lived odd-odd isotope to be measured, facing the first anode. The middle plate served as a compensation cathode, operated at  $-400$  V, to balance the beta-gamma background for the short-lived sample. After the samples were deposited in the chamber, it was filled with 1 Los Alamos atm pressure of methane gas ( $\sim 580$  mm of mercury).

The data were collected as event addresses in a two-dimensional array of pulse height and neutron time of flight. The data were read out every hour to permit optimization of the counting loss correction, statistical weighting of partial runs, and decay and buildup of isotopes in the sample during the run. The  $^{235}\text{U}$  fission rate served only as a relative intensity and flux-shape monitor. The cross section of  $^{232}\text{Pa}$  was determined relative to that of  $^{233}\text{U}$  and that of  $^{238}\text{Np}$  was determined relative to  $^{239}\text{Pu}$ , which grew into the samples as the contaminants  $^{233}\text{Pa}$  and  $^{239}\text{Np}$  decayed.

The successful run to produce  $^{232}\text{Pa}$  took  $\sim 39$  h of 17-MeV deuteron irradiation at an average current of  $5.2 \mu\text{A}$ . The sample thickness was 0.0508 cm (20 mil)

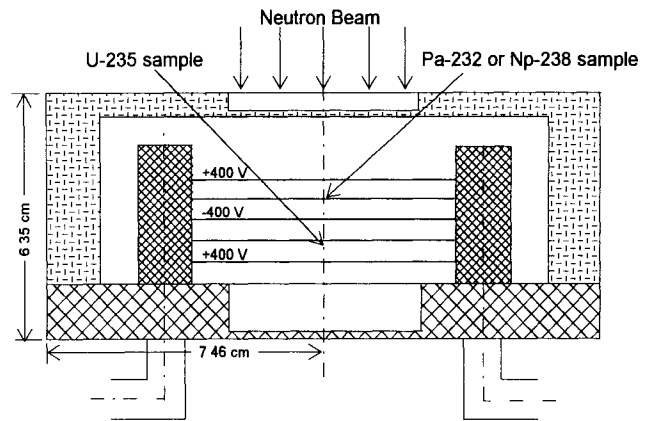


Fig. 3. A sketch of the fission chamber showing the sample locations.

of thorium, with  $1.27 \times 10^{-3}$  cm (0.5 mil) aluminum coating on both sides. At the end of this run, it was estimated from the measured cross section and the deuteron beam intensity that the thorium target contained  $\sim 90$  ng of  $^{232}\text{Pa}$ . The irradiated thorium target was removed from the IBF beamline, packed, and shipped to a hot cell in the Chemistry-Metallurgy Research building where the radiochemical separation was done. The separation of  $^{232}\text{Pa}$  took  $\sim 9$  h. At the end of the process, the  $^{232}\text{Pa}$  was deposited on the fission foil backing and assembled into the fission chamber. The fission chamber was shipped to the LANSCE facility where it was unpacked, inserted into the beamline, connected to the electronics and filled with 1 atm of methane gas. At that time, it was estimated that there were 30 ng of  $^{232}\text{Pa}$  and 100 ng of  $^{233}\text{Pa}$  in the fission chamber. Data were collected for 99 h, by that time 88% of the  $^{232}\text{Pa}$  in the chamber had decayed.

The procedure for  $^{238}\text{Np}$  samples followed a very similar pattern with one extra complication. In the separation of neptunium from uranium, it was found that extreme care was needed to avoid the presence of  $^{235}\text{U}$  in the fissile deposit; even a trace amount could compromise the quality of the  $^{238}\text{Np}$  data. The two samples of  $^{238}\text{Np}$  contained  $\sim 10$  ng of  $^{238}\text{Np}$  and 40 ng of  $^{239}\text{Np}$  at the beginning of the data collection.

The 11-ng  $^{236}\text{Np}$  sample was deposited in the fission chamber with the 400-ng  $^{235}\text{U}$  sample. In this case, the uranium sample was used to normalize the data under the assumption that both parts of the fission chamber had the same efficiency. Dry runs were also made with a sample of  $11 \mu\text{g}$   $^{237}\text{Np}$ , which gave an independent check of the validity of this assumption.

### IV. DATA REDUCTION

The data analysis of the  $^{238}\text{Np}$  and  $^{232}\text{Pa}$  samples is much more complicated than the analysis of the

<sup>a</sup>The fission foil was made available to us by D. W. Efurud.

$^{236}\text{Np}$  sample, because of the fast decay of the samples. The  $^{236}\text{Np}$  sample was simply normalized to the  $^{235}\text{U}$  sample and corrected for the small flight path difference, according to the following expression:

$$\sigma_f^{236}(E_i) = \frac{400 \text{ ng}}{11 \text{ ng}} \frac{236}{235} \left( \frac{5.184 \text{ m}}{5.194 \text{ m}} \right)^2 \times \frac{\phi(0.0253)}{\phi(E)_i} \frac{C^{236}(E_i)}{C^{235}(0.0253)}, \quad (1)$$

where  $C^x(E_i)$  denotes the counts of sample  $x$  at energy  $E_i$ .

The nature of the two other measurements was similar. In both cases, a very short-life isotope,  $^{232}\text{Pa}$  or  $^{238}\text{Np}$ , is present in the sample in a small amount,  $\sim 10$  to  $30$  ng. The isotopes decay by beta emission to  $^{232}\text{U}$  and  $^{238}\text{Pu}$ , respectively, both having small known fission cross sections. The samples also contained contamination of  $^{233}\text{Pa}$  and  $^{239}\text{Np}$ , respectively, with a number of atoms that were three to four times higher than the isotopes of interest. These contaminants have small thermal and resonance fission cross sections, but decay by beta emission to  $^{233}\text{U}$  and  $^{239}\text{Pu}$  with large fission cross sections. Therefore, the buildup of fissionable material in the sample as a function of time cannot be ignored and must be corrected properly.

Another complication in the data reduction is the fact that the LANSCE flux cannot be taken as constant in time. Because of the short half-life of the isotopes of interest the first 48 h of data acquisition were critical. The data acquisition was done in runs of 1 h each, and data were recorded regardless of the quality of the LANSCE neutron beam. A problem can arise if the PSR or the LAMPF accelerator does not operate during part of a 1-h run or if the beam intensity changes between runs. The data reduction procedure assumes that the LANSCE flux can be taken as constant over a 1-h run. This procedure averages the beam fluctuations over a 1-h run and properly treats beam fluctuations between runs.

#### IV.A. Reaction Rates

The derivation of the reaction rate equation in each channel is shown here for  $^{232}\text{Pa}$ . The derivation for the  $^{238}\text{Np}$  reaction rate is similar, and only the final expression will be given. The assumptions made in the derivation of the reaction equations are the following:

1. The flux  $\phi_i$  in channel  $i$  is constant in each 1-h run.

2. The number of atoms of  $^{232}\text{Pa}$  and  $^{233}\text{Pa}$  can be treated constant during a 1-h run; these are  $^{232}N(t)$  and  $^{233}N(t)$ , respectively, where  $t$  is the time from the end of the radiochemical separation process to the effective center of the 1-h run.

3. The energy-dependent neutron flux shape is known. The flux shape was measured with a  $^6\text{Li}$  mon-

itor located in the same beamline at a flight path of  $\sim 7$  m. Small changes in the thermal Maxwellian and  $1/E$  spectrum were monitored during each run by the  $^{235}\text{U}$  monitor.

The count rate of channel  $i$  in the  $^{235}\text{U}$  chamber as a function of the time of flight  $t$  is given by

$$\dot{C}_i^{235}(t) = N^{235} \eta p(t) \phi_i \sigma_f^{235}(E_i), \quad (2)$$

where

$N^{235}$  = number of  $^{235}\text{U}$  atoms in the sample

$\eta$  = fission detection efficiency

$p(t)$  = time-dependent flux intensity factor

$\phi_i$  = flux intensity at channel  $i$  (the energy-dependent flux shape)

$\sigma_i^{235}(E_i)$  = fission cross section of  $^{235}\text{U}$  at energy  $E_i$ .

Equation (2) can be integrated between  $t_1$  and  $t_2$ , where  $t_2 - t_1$  correspond to a 1-h run:

$$\int_{t_1}^{t_2} \dot{C}_i^{235}(t) dt = C_{i,r}^{235} = N^{235} \eta \phi_i \sigma_f^{235}(E_i) \int_{t_1}^{t_2} p(t) dt. \quad (3)$$

The measured  $^{232}\text{Pa}$  fission cross section can be normalized to the  $^{235}\text{U}$  sample, which also served as a monitor. The normalization can be done at 0.0253 eV or to the  $^{235}\text{U}$  cross-section integral between  $E_1 = 7.8$  to  $E_2 = 11$  eV. Equation (4) assumes the normalization is done by integration between channels  $I_1$  and  $I_2$ , which correspond to energy  $E_1$  and  $E_2$ :

$$\int_{t_1}^{t_2} p(t) dt = \frac{\sum_{j=I_1}^{I_2} C_{j,r}^{235}}{N^{235} \eta \sum_{j=I_1}^{I_2} \phi_j \sigma_j^{235}(E_j)}. \quad (4)$$

The reaction equation for the  $^{232}\text{Pa}$  chamber is calculated in the same way but also includes the time-dependent decay and buildup of the isotopes in the sample:

$$\begin{aligned} \dot{C}_i^{232}(t) = & \eta k(t) \phi_i N^{232}(0) \\ & \times \left[ e^{-\lambda^{232}t} \sigma_i^{232\text{Pa}} + (1 - e^{-\lambda^{232}t}) \sigma_i^{232\text{U}} \right. \\ & + \frac{N^{233}(0)}{N^{232}(0)} e^{-\lambda^{233}t} \sigma_i^{233\text{Pa}} \\ & \left. + \frac{N^{233}(0)}{N^{232}(0)} (1 - e^{-\lambda^{233}t}) \sigma_i^{233\text{U}} \right]. \quad (5) \end{aligned}$$

There are no measurements of the energy-dependent cross section of  $^{233}\text{Pa}$ . The thermal value is estimated to be  $< 0.1$  b; therefore, the term for the fission of

$^{233}\text{Pa}$  was ignored. Integrating and substituting Eq. (4) gives

$$\int_{t_1}^{t_2} \dot{C}_i^{232}(t) dt = \frac{\sum_{j=I_1}^{I_2} C_{j,r}^{235}}{N^{235} \eta \sum_{j=I_1}^{I_2} \phi_j \sigma_j^{235}(E_j)} \frac{N^{232}(0)}{N^{235}} \times \phi_i \left[ e^{-\lambda^{232} t} \sigma_i^{232\text{Pa}} + (1 - e^{-\lambda^{232} t}) \sigma_i^{232\text{U}} + \frac{N^{233}(0)}{N^{232}(0)} (1 - e^{-\lambda^{233} t}) \sigma_i^{233\text{U}} \right]. \quad (6)$$

By rearranging and substituting the time integral with the number of counts in a 1-h run noted  $r$ , at channel  $i$ , the  $^{232}\text{Pa}$  fission cross section for a 1-h run is given by

$$\sigma_{i,r}^{232} = \left[ C_{i,r}^{232} \frac{\sum_{j=I_1}^{I_2} \phi_j \sigma_j^{235}(E_j)}{\sum_{j=I_1}^{I_2} C_{j,r}^{235}} \frac{N^{235}}{N^{232}(0) \phi_i} - (1 - e^{-\lambda^{232} t}) \sigma_i^{232\text{U}} - \frac{N^{233}(0)}{N^{232}(0)} (1 - e^{-\lambda^{233} t}) \sigma_i^{233\text{U}} \right] e^{\lambda^{232} t}. \quad (7)$$

The result of Eq. (6) is the  $^{232}\text{Pa}$ -averaged cross section for a 1-h run. Next, to be proportional to the amount of sample, a weighed average on all the 1-h runs was calculated. The weight was chosen such that the first runs, when the samples are fresh, have more weight. To remove the effects of runs with poor counting statistics, the cross section was also weighted by the normalization integral of the  $^{235}\text{U}$  monitor. The weight is given by

$$w_r = e^{-2^{232} \lambda t_r} \sum_{i=I_1}^{I_2} C_{i,r}^{235}, \quad (8)$$

and the averaged fission cross section is given by

$$\sigma_i^{232} = \frac{\sum_{r=1}^n w_r \sigma_{i,r}^{232}}{\sum_{r=1}^n w_r}. \quad (9)$$

The same procedure was done for the  $^{238}\text{Np}$  sample, and the final expression for the fission cross section of a 1-h run is given by

$$\sigma_{i,r}^{238} = \left[ C_{i,r}^{238} \frac{\sum_{i=I_1}^{I_2} \phi_i \sigma_i^{235}(E_i)}{\sum_{i=I_1}^{I_2} C_{i,r}^{235}} \frac{N^{235}}{N^{238}(0) \phi_i} - (1 - e^{-\lambda^{238} t}) \sigma_i^{238\text{Pu}} - \frac{N^{239}(0)}{N^{238}(0)} (1 - e^{-\lambda^{239} t}) \sigma_i^{239\text{Pu}} \right] e^{\lambda^{238} t}. \quad (10)$$

To make Eqs. (7) and (10) valid, the  $^{232}\text{U}$ ,  $^{233}\text{U}$ ,  $^{238}\text{Pu}$ , and  $^{239}\text{Pu}$  fission cross sections must have the same resolution as the measured  $^{232}\text{Pa}$  and  $^{238}\text{Np}$  cross sections. The ENDF/B-VI cross sections were broadened with a Gaussian. The Gaussian width as a function of the energy is given by

$$fwhm(E) = \frac{2}{72.3L} \left\{ E^3 \left[ \left( \frac{\Delta t}{E^p} \right)^2 + pw^2 \right] \right\}^{1/2}, \quad (11)$$

where

$L$  = flight path (5.194 m for the  $^{235}\text{U}$  chamber and 5.184 m for the sample chamber)

$\Delta t$  = contribution of the moderator ( $\mu\text{s}$ )

$pw$  = contribution of LANSCE pulse width ( $\mu\text{s}$ ).

The power  $P$  was used to obtain a better fit. The optimal broadening parameters  $\Delta t = 4.5$ ,  $pw = 0.25$ , and  $p = 0.6$  were obtained by broadening the ENDF/B-VI  $^{235}\text{U}$  fission cross section to agree with the measured  $^{235}\text{U}$  cross section.

The data-reduction procedure started by first correcting each run for dead time and then calculating the 1-h fission cross section. These cross sections were averaged according to Eq. (9) to give the final cross section. The FORTRAN program used for these calculations was also coded with equations for the error propagation assuming independent error analysis. Therefore, along with the final cross section, an estimated error was also calculated.

Note that the data-reduction procedure is valid even though there were no accurate values for the number of  $^{232}\text{Pa}$ ,  $^{238}\text{Np}$ , and  $^{235}\text{U}$  atoms at the time of separation. The only quantity required is the ratio of  $^{233}\text{Pa}$  to  $^{232}\text{Pa}$  and  $^{239}\text{Np}$  to  $^{238}\text{Np}$ . This ratio was obtained by gamma counting of the sample deposit after the radiochemical separation process and was found to be  $4.21 \pm 0.17$  and  $5.03 \pm 0.075$ , respectively. To use this information, the data reduction program was executed several times, each time changing the atom ratio of  $^{235}\text{U}$  to  $^{232}\text{Pa}$  around the assumed value. The objective was to get zero cross section in the vicinity of strong  $^{233}\text{U}$  resonances. This procedure essentially uses the buildup of unwanted isotopes in the sample to determine the number of atoms in the sample of interest.

A similar procedure was done for  $^{238}\text{Np}$  with  $^{239}\text{Pu}$  resonances.

## V. RESULTS

### V.A. Neptunium-238

The fission cross section of  $^{238}\text{Np}$  was obtained by combining forty-two 1-h runs. The cross section was grouped to macro channels to improve the counting statistics and is plotted in Fig. 4. The biggest contribution to the low energy cross section is from the resonance at 1.1 eV with an area of  $621 \pm 30 \text{ b}\cdot\text{eV}$ . The poor counting statistics and plutonium resonances make it hard to isolate more resonances above 1.1 eV. The cross section has an overall  $1/v$  shape with a thermal value of  $2641 \pm 58 \text{ b}$ . This value is not in agreement with the value of  $2070 \pm 30 \text{ b}$  quoted by Spencer and Baumann<sup>4</sup> or with the  $2110 \pm 74 \text{ b}$  measured by Abramovich et al.<sup>5</sup> The fission resonance integral between 0.5 to 500 eV is  $1379 \pm 30 \text{ b}$ , which is also not in agreement with the value of 880 b reported by Spencer and Baumann. Abramovich et al. reported the resonance integral as  $905 \pm 48 \text{ b}$ , which agrees with the measurement of Spencer and Baumann. These two resonance integral measurements were done with the cadmium cover method, while our measurement is an integral of the pointwise cross section.

### V.B. Protactinium-232

The  $^{232}\text{Pa}$  fission cross section is plotted in Fig. 5. The  $^{232}\text{Pa}$  shows more structure than  $^{238}\text{Np}$ . There are

two strong resonances, at 0.33 and 2.73 eV and several smaller resonances. The thermal fission cross section was found to be  $1506 \pm 14$  and the resonance integral from 0.5 to 500 eV is  $1075 \pm 11 \text{ b}$ . The thermal cross section is a factor of two higher than the value quoted by Mughabghab, Divadeenam, and Holden.<sup>6</sup> However, the reference to this value is a private communication and it is not known how this value was obtained. Our data were fitted with single-level Breit-Wigner parameters listed in Table I, and the measured and fitted cross section are plotted in Fig. 6. The statistical  $g$  factor was chosen as 0.5 for all resonances. The fit was

TABLE I  
Single-Level Breit-Wigner Resonance  
Parameters of  $^{232}\text{Pa}$

$E_0$ (eV)	$2g\Gamma_n$ (meV)	$\Gamma_f$ (meV)
-5.00	13.645	844.7
0.33	0.142	202.2
0.67	0.054	207.7
1.37	0.053	462.1
2.73	0.335	237.3
3.06	0.164	275.2
4.14	0.224	409.4
6.44	0.179	268.6
7.45	0.086	486.3
8.41	0.115	479.1
8.85	0.288	412.8

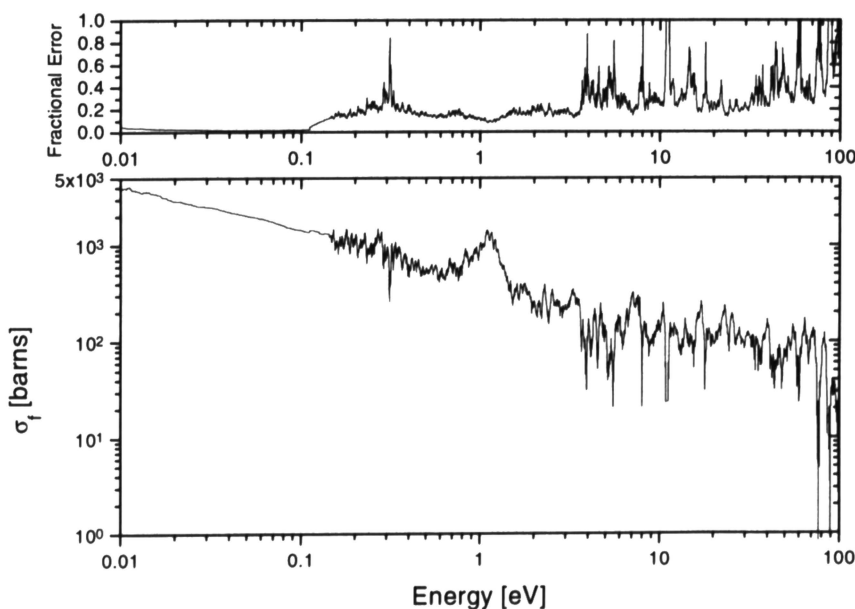


Fig. 4. The fission cross section of  $^{238}\text{Np}$ . Also shown are the fractional errors associated with each point.

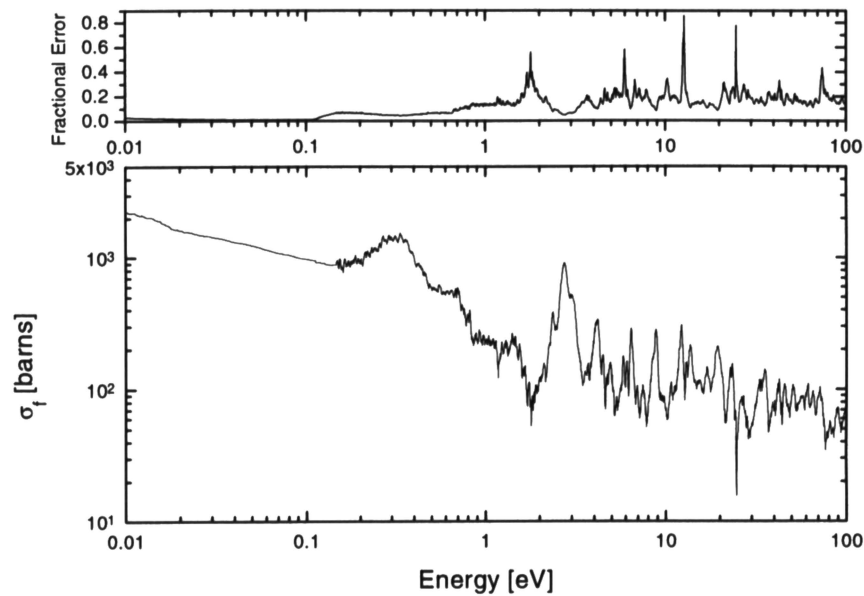


Fig. 5. The fission cross section of  $^{232}\text{Pa}$ . Also shown are the fractional errors associated with each point.

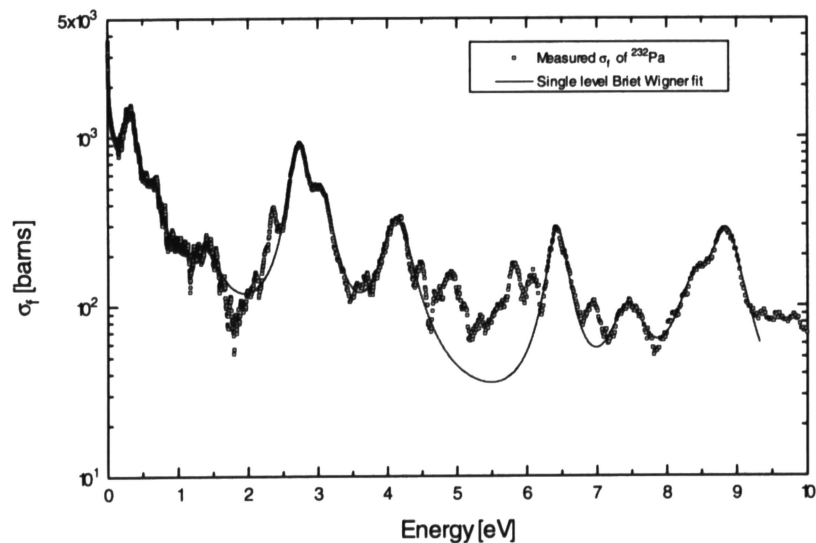


Fig. 6. Measured and fitted fission cross section of  $^{232}\text{Pa}$ . The parameters used for the Breit-Wigner fit are listed in Table I.

done in regions to preserve the area under each resonance rather than providing an overall fit that will tend to give broader widths and fit the area between resonances better. The fit indicates that there are some missing levels in regions that have poor counting statistics because of corrections for  $^{233}\text{U}$  and the 6 eV resonance in  $^{232}\text{U}$ . In these regions, it was not possible to distinguish structure from correction errors. Also, above 10 eV, it was not possible to clearly resolve resonances from statistical fluctuations created when correcting for

the uranium isotopes. Overall, the cross section has a  $1/v$  shape as expected.

#### *V.C. Neptunium-236*

A total of  $\sim 30$  h of data was collected, and the fission cross section was then calculated using Eq. (1). Valkiy et al.<sup>7</sup> reported on measurements of  $^{236}\text{Np}$  using a lead spectrometer and a monochromator. In Fig. 7, our measured fission cross section is plotted with the

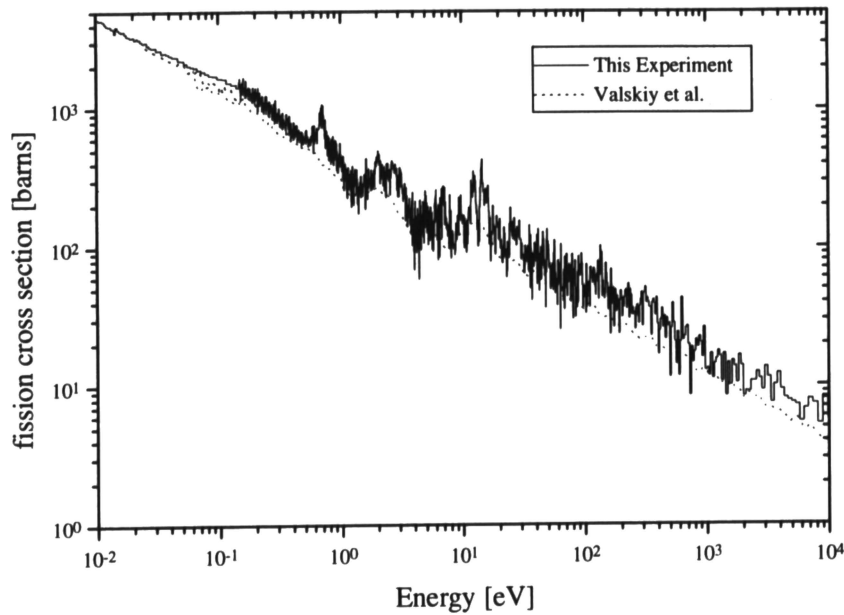


Fig. 7. Measured fission cross section of  $^{236}\text{Np}$  and the measurement of Valskiy et al.

measurements of Valskiy et al. Two curves were plotted for the data of Valskiy et al., one for the lead spectrometer data and the other for a thermal measurement. The shape of the two cross sections is in good agreement. Our measurement is  $\sim 20\%$  higher over all energies and has much higher resolution. The counting statistics were good enough to fit the resonance structure up to 25 eV. The data were fitted using the SAMMY

code and were treated with a simple Breit-Wigner formula. The resonance parameters are listed in Table II, and the fits are plotted in Fig. 8. The average level spacing  $\langle D \rangle = 3.79$  eV and the average fission width  $\langle \Gamma_f \rangle = 0.586$  eV give 3.8 for the number of effective channels [ $N_{eff} = 2\pi(\langle \Gamma_f \rangle / \langle D \rangle)$ ]. This number is an underestimate because several observed resonances are expected to be clusters of resonances that cannot be

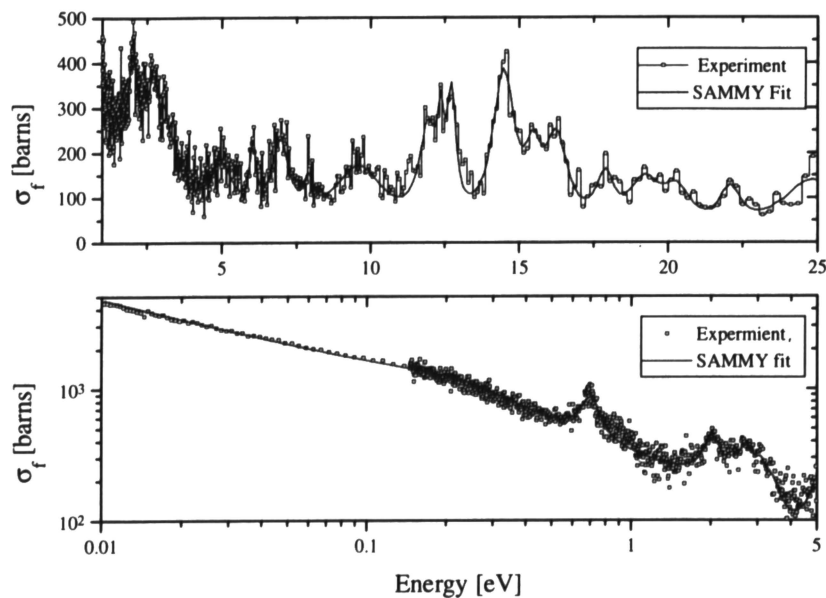


Fig. 8. Fitted  $^{236}\text{Np}$  fission cross section. The upper curve shows the higher energy region and the lower curve shows the thermal region. The resonance parameters are listed in Table II.



TABLE II  
Single-Level Breit-Wigner Resonance  
Parameters of  $^{236}\text{Np}$

$E_0$ (eV)	$2g\Gamma_n$ (meV)	$\Gamma_f$ (meV)
-1.41	2.624	7006.0
0.20	0.033	337.7
0.70	0.055	89.2
2.03	0.173	341.2
2.39	0.069	190.7
2.67	0.146	280.5
2.80	0.114	269.5
3.07	0.138	293.4
3.38	0.139	473.9
4.99	0.434	915.2
6.03	0.219	196.7
6.96	0.693	646.3
7.90	0.186	293.2
9.62	2.224	2036.6
11.95	1.553	675.0
12.36	0.570	114.2
12.72	1.127	277.6
14.48	3.628	839.4
15.47	1.090	549.0
16.25	2.442	876.8
17.88	1.201	651.7
19.20	2.045	1198.5
20.28	1.703	1142.8
22.08	1.367	783.0

resolved. The measured thermal value at 0.0253 eV was found to be  $3007 \pm 90$  b; this value is 8.6% higher than the value of  $2770 \pm 260$  obtained by Valskiy et al. but is in agreement within the quoted error of both experiments. The resonance integral from 0.5 to 10 000 eV was calculated to be  $1353 \pm 86$  b, which is ~30% higher than the value of  $1040 \pm 60$  measured by Valskiy et al. Most of the differences are above the thermal region and appear to be systematic, the same percent over all energies.

## VI. CONCLUSIONS

The fission cross sections of the 1.31-day  $^{232}\text{Pa}$  and 2.117-day  $^{238}\text{Np}$  odd-odd isotopes were measured in a time-of-flight experiment. The samples have very short half-lives, which complicated every phase of the experiment. The method of producing, separating, and measuring the sample, with the ( $d,2n$ ) reaction, all in the same laboratory proved to work well. It was very important to keep the time between the end of sample production and chemistry phase short so that the sample was not lost by decay. It was also important to keep

the radiochemistry yield as high as possible and to make sure that contaminants such as  $^{235}\text{U}$  are not in the sample. The data were collected in 1-h files that helped reduce the effects of varying flux and machine downtime on the cross section. It also helped us to weight the data by the decay time, in order to reduce the effects of isotopes with high fission cross section that were building up in the sample.

The fission cross section of  $^{236}\text{Np}$  was measured in the same system. The resolution of the system was good enough to resolve much structure, and resonance parameters were obtained by fitting the data. It seems that the number of open channels in  $^{236}\text{Np}$  is higher than 3.8 eV as might be expected for an odd-odd nuclide.

It is interesting to compare the measurements of odd-odd nuclides with the fission cross-section measurements<sup>8</sup> of  $^{254}\text{Es}$ . In the case of  $^{254}\text{Es}$ , structure was not resolved, which indicated a combination of low average level spacing and large fission widths resulting from many open channels. In the isotopes reported here and also in  $^{242}\text{Am}$  reported by Browne et al.,<sup>9</sup> the fission cross-section structure is clearly resolved and has perhaps 4 to 6 open channels.

Finally, we need to address the question: "Why are the fission cross sections determined in the present measurement systematically 20 to 30% higher than all other data?" The answer is that we do not know. In the case of  $^{236}\text{Np}$ , the answer might well be that we had more sample material deposited on the foil than we thought; in this case, an uncertainty of  $\pm 20\%$  in the number of atoms in the deposit is not unexpected, and the agreement in the case of the 11- $\mu\text{g}$   $^{237}\text{Np}$  sample says nothing about  $^{236}\text{Np}$ . But for the  $^{232}\text{Pa}$  and  $^{238}\text{Np}$ , the cross sections are normalized to the well-known resonances in  $^{233}\text{U}$  and  $^{239}\text{Pu}$ . The sample thicknesses are the same; it is the same sample. The decay constants of  $^{233}\text{Pa}$  and  $^{239}\text{Pu}$  are well known, and the germanium-lithium gamma-spectrometer determination of the atom ratios of  $^{233}\text{Pa}/^{232}\text{Pa}$  and  $^{239}\text{Np}/^{238}\text{Np}$  is a well-established technique at LANL, giving results with a far higher accuracy than  $\pm 25\%$ , on a routine basis.

There is one possible explanation that we were not able to investigate because of a lack of running time at the LANSCE facility: Perhaps there is some kind of off-energy neutron background underlying the observed fission structure. Our normalization to  $^{233}\text{U}$  and  $^{239}\text{Pu}$  was done to the resonance structure with an incompletely decayed sample. If there were an off-energy neutron background, it would not have been readily observed, until the samples had completely decayed. But the 1993 LANSCE run cycle ended while the samples were still comparatively fresh. We planned to rerun the same fission chamber during the 1994 cycle, but there was no LANSCE cycle in 1994. And unfortunately, by 1995, the experimental arrangement had been compromised, the research team had been disbanded, and the work was no longer funded. Therefore, in this paper, we report what we observed.

## ACKNOWLEDGMENT

The authors owe D. W. Efurud a debt of gratitude for providing us the opportunity to make the fission measurements on long-lived  $^{236}\text{Np}$ .

## REFERENCES

1. C. D. BOWMAN et al., "Nuclear Energy Generation and Waste Transmutation Using an Accelerator-Driven Intense Thermal Neutron Source," *Nucl. Instrum. Methods*, **A320**, 336 (1992).
2. M. S. MOORE et al., "Development of a Technique for Measuring Fission Cross Sections of Interest to Accelerator Transmutation of Waste (ATW)," Int. Conf. Nuclear Data for Science and Technology, Gatlinburg, Tennessee, May 1994.
3. M. S. MOORE and Y. DANON, "Resonance Enhancement in the Accelerator Transmutation of 1.3-Day  $^{232}\text{Pa}$  and 21-Day  $^{238}\text{Pa}$ ," Int. Conf. Accelerator-Driven Transmutation Technologies and Applications, Las Vegas, Nevada, July 25-29, 1994.
4. J. D. SPENCER and N. P. BAUMANN, "Measurement of Integral Fission Cross Sections for  $^{238}\text{Np}$ ," *Trans. Am. Nucl. Soc.*, **12**, 284 (1969).
5. S. ABRAMOVICH et al., "Integral Neutron Fission Cross-Section Measurement for Np-238 Near the Thermal Point" (to be published).
6. S. F. MUGHABGHAB, M. DIVADEENAM, and N. E. HOLDEN, *Neutron Cross Sections*, Academic Press (1984).
7. G. V. VALSKIY et al., "The Fission Cross Section of  $^{236}\text{Np}$  with Neutron Energies up to 10 keV" (in Russian).
8. Y. DANON, N. W. HILL, R. W. HOFF, R. W. LOUGHEED, P. E. KOEHLER, and M. S. MOORE, "Measurement and Analysis of the Neutron-Induced Fission Cross Section of  $^{247}\text{Cm}$ ,  $^{250}\text{Cf}$  and  $^{254}\text{Es}$ ," Int. Conf. Nuclear Data for Science and Technology, Gatlinburg, Tennessee, May 1994.
9. J. C. BROWN, R. M. WHITE, R. E. HOWE, J. H. LANDRUM, R. J. DOUGAN, and R. J. DUPZYK, " $^{242m}\text{Am}$  Fission Cross Section," *Phys. Rev. C*, **29**, 6, 2188 (1984).